

Rheology Study in Polyurethane Rigid Foams

Lifeng Wu, Janine Van Gemert, Rafael E. Camargo

*Huntsman Corporation
2190 Executive Hills Blvd.
Auburn Hills, MI 48326
USA*

ABSTRACT

The use of polyurethane (PU) rigid foam has been growing rapidly in many industries due to its excellent combination of energy conservation, good mechanical strength with lighter weight than other traditional materials. In this work, glass transition temperature was studied using rheology for a PU rigid foam model system. Some structure-property correlations have been established based on effects of crosslink density, aromaticity, plasticizer, and index. As demonstrated in some real examples, this understanding provides some guidelines in choosing the right ingredients to achieve certain properties, and therefore significantly accelerates the development of new PU rigid systems. In addition, rheology data also revealed an interaction between glass transition and the extent of curing for molded PU foams, indicating the significance of reactivity and processability to achieve desired end properties.

INTRODUCTION

The soaring price of crude oil has made energy conservation increasingly important. As the most efficient and practical thermal insulating materials, polyurethane (PU) rigid foams play a very important role in modern construction and other industrial applications. Besides its low thermal conductivity, which is mainly due to blowing agent and fine closed cell structure, PU rigid foam offers good adhesion to facing materials, good dimensional stability, and excellent mechanical strength at low densities [1]. These features are primarily derived from a highly crosslinked network structure in the PU matrix. The majority of PU rigid foams are prepared by mixing diphenylmethane diisocyanate (MDI) or its derivatives with a polyol blend which contains polyols, blowing agents, surfactants, catalysts, and other additives such as, flame retardants. Polymeric MDI is most commonly used to make PU rigid foams, while a very broad range of polyols can be selected to achieve different end properties. Therefore, understanding the fundamentals of structure-property relationships can greatly help formulators to identify and optimize combinations of various raw materials.

This paper focuses on the effect of polymer structure on glass transition temperature (T_g) of PU rigid foams. As stated by Hiemenz and Lodge [2], “the value of T_g is the single most important characteristic in choosing a polymer for a given application”. For instance, T_g can be used to define the upper limit of service temperature for PU rigid foam. As illustrated in Figure 1, a typical PU foam can undergo a significant change in mechanical strength (i.e., flexural or shear modulus) as the temperature is increased to around T_g , which indicates a transition from rigid to rubbery material. This behavior suggests that PU rigid foam should be applied below its T_g in order to behave as a rigid material. Furthermore, the value of T_g reflects the rigidity of polymer matrix, which impacts mechanical strength, dimensional stability, long term aging behavior, and other properties. Therefore, understanding the relationship between structure and T_g can considerably accelerate the development of new systems.

Unlike melting temperature, which is a thermodynamic property of solid material, T_g is a dynamic property for amorphous polymers and it is related to relaxation behavior of local chain segments. As a result, T_g depends on the following factors affecting the mobility of chain segments: crosslink density in the network structure, aromaticity (Ar, weight fraction of aromatic structures in the polymer matrix), polyisocyanurate (PIR) content, plasticizer concentration, and so on. Due to its dynamic attribute, for a given polymer, T_g can adopt a range of values identified using various characterization techniques such as dilatometry, differential scanning calorimetry (DSC), and dynamic mechanical thermal analysis (DMTA). In this work, DMTA was used to locate T_g using a typical shear rheometer. Details about DMTA parameters and their interpretation can be found elsewhere [3, 4]. Figure 1 showed that the glass transition induced a large change in rheological properties: precipitous drop in storage modulus (G'), a small peak of loss modulus (G''), and a sharp peak of loss tangent

($\text{Tan}(\delta)$). Although all these three features can be used to locate T_g , the peak of $\text{Tan}(\delta)$ was used in this study because it is easier to identify with less error than using the other two parameters. T_g was investigated as a function of crosslink density, aromaticity, plasticizer concentration, PIR content, and processing conditions for a water-blown PU model system. Structure-property correlations were established for this model system and verified with some real examples.

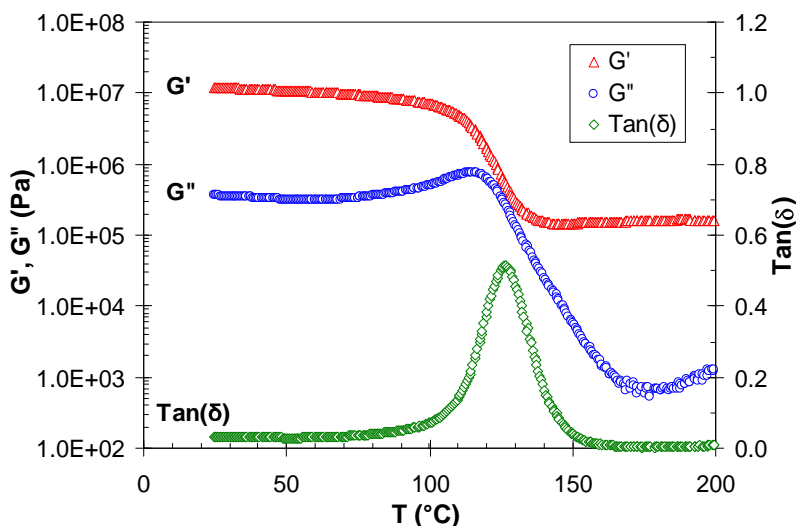


Figure 1. Representative DMTA curves for a PU rigid foam.

EXPERIMENTAL

Materials

Seven blended polyols, A to G, were prepared from individual propylene oxide (PO) based Huntsman polyols to achieve certain average molecular weights (M_c) between crosslinks and aromatic contents (Ar). Two catalyst packages were applied: catalyst I yields balanced gel and blow reactions, while catalyst II can further catalyze the PIR reaction. All polyol blends were combined with RUBINATE[®] M polymeric MDI ($\text{NCO}_v = 31.2$, $F_n = 2.7$) to make PU rigid foams. FYROL[®] PCF (i.e., Tris(chloroisopropyl) phosphate, TCPP) was used as a plasticizer. It was obtained from Supresta. A standard rigid foam silicone surfactant was supplied by Evonik Degussa.

Foam preparation

100 grams of polyol blend was mixed with the required amount of RUBINATE[®] M isocyanate for 10 seconds at 2000 rpm. Then the mixture was poured into a 32oz paper cup to make a free rise foam. Foam density was measured from the foam in the cup by cutting the top off and comparing the weight to that of a water filled cup. Rectangular bar specimens ($0.5\text{cm} \times 1.0\text{cm} \times 5.0\text{cm}$) were cut near the center of foam for rheology measurement.

Rheology measurement

DMTA measurement was conducted on a stress-controlled AR-2000 rheometer (TA Instruments). Under dynamic mode, sinusoidal shear stress with a certain frequency was applied on a specimen by a motor, while the response strain was monitored by a displacement sensor. How a material responds to a dynamic stress depends on its own viscoelasticity [3, 4]. An elastic material shows a sinusoidal strain response without any phase lag compared to the applied stress curve, while a viscous material yields a strain response with 90° phase lag. For a typical viscoelastic material, the strain response has a phase lag between 0 and 90° . This phase lag is referred to as phase angle (δ). The response can be resolved into two components: one is elastic (or storage) component with 0 phase angle, the other is viscous (or loss) component with 90° phase angle. As a result, viscoelastic properties can be characterized by three variables: storage shear modulus (G'), loss shear modulus (G''), and phase angle (δ). In general, loss tangent $\text{Tan}(\delta) = G''/G'$. All DMTA data were collected for foam specimens at a temperature ramp rate of $3^\circ\text{C}/\text{min}$ with 0.2% strain and 1 Hz frequency.

RESULTS AND DISCUSSION

1) Effect of crosslink density

The effect of crosslink density was studied for Formulations 1 to 3 (Table 1). Average functionality (F_{n_polyol}) of blended polyols A to C was varied from 4.7 to 3.0 while keeping a constant average hydroxyl value, OH_v (403 mgKOH/g). Index was chosen as 100 to avoid unreacted dangling chains and any other structures such as allophanate, biuret, carbodiimide or polyisocyanurate (PIR). As designed, overall aromaticity calculated from the amount of isocyanate, was the same (29.5%) for those three formulations (Table 1). As shown in Figure 2, decreasing functionality of the polyol shifted T_g to lower temperature due to the reduction of crosslink density. Since the same water content led to similar cup foam densities (about 7 pcf), the change of rubbery plateau modulus (above T_g) can also be associated with the difference in crosslink density. Values of T_g were determined using the peak of $Tan(\delta)$, and these were tabulated in Table 1.

Formulations	1	2	3	4	5	6
Polyol A	96.2					
Polyol B		96.2				
Polyol C			96.2			
Polyol D				96.2		
Polyol E					96.2	
Polyol F						96.2
Catalyst I	2.0	2.0	2.0	2.0	2.0	2.0
Surfactant	1.0	1.0	1.0	1.0	1.0	1.0
Water	0.8	0.8	0.8	0.8	0.8	0.8
Index	100	100	100	100	100	100
OH_v (mgKOH/g)	403	403	403	445	527	638
F_{n_polyol}	4.7	4.0	3.0	4.2	3.7	3.3
M_c (g/mol)	360	390	496	360	360	360
Aromaticity	29.5%	29.5%	29.5%	31.0%	33.5%	36.3%
T_g (°C)	127	116	97	131	143	151

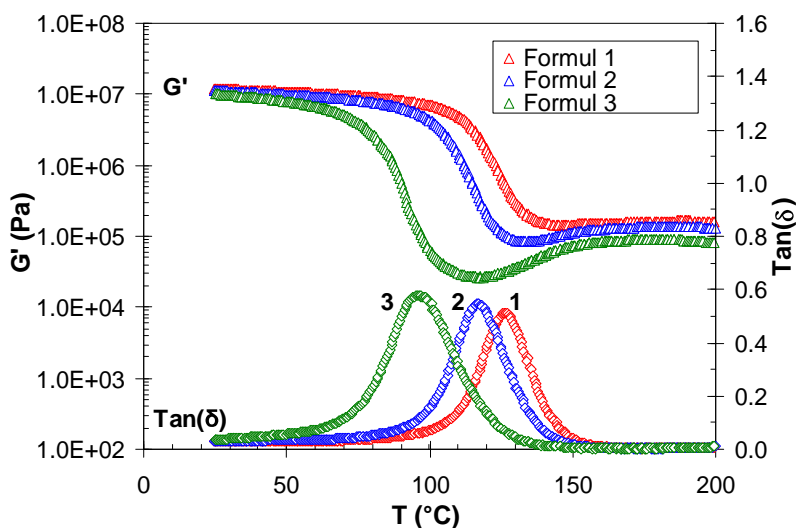


Figure 2. DMTA curves of Formulations 1 (red), 2 (blue) and 3 (green).

To further analyze the data, we calculated average molecular weight (M_c) between crosslinks, which is inversely proportional to crosslink density. There are at least two ways to calculate M_c : one is to divide the total weight of polymer matrix by moles of crosslinks; the other is to divide total weight of polymer matrix by moles of chain branches. The first one can not differentiate the functionality of crosslinker ($F_n \geq 3$), while the second one can. Since the functionality of crosslinker does impact the mobility of chain segments and consequently T_g , the second method was chosen to determine the value of M_c in this work (Table 1). Figure 3 shows a simple linear relationship between T_g and crosslink density represented below by $1/M_c$:

$$T_g (\text{°C}) = 38.334 \times 10^3 / M_c + 19.2 \quad (1)$$

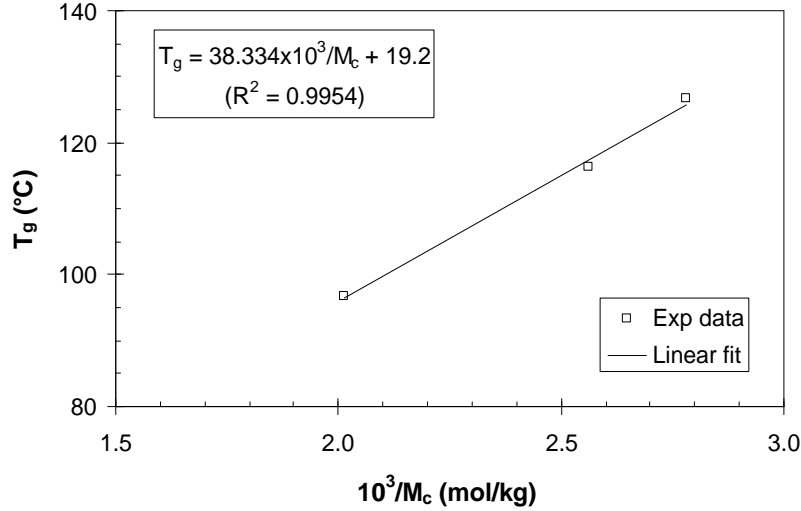


Figure 3. Glass transition temperature (T_g) as a function of crosslink density ($1/M_c$). Open squares denote experimental data, while solid straight line denotes linear fit of experimental data.

Interestingly, T_g of un-crosslinked linear polymers also depends linearly on molecular weight, which can be explained by a free volume argument [2]. Similarly for this model system, smaller M_c (or tighter crosslinked network structure) results in less free volume for chain segment to relax and therefore higher T_g . Furthermore, we can consider the network structure as a binary blend of linear chains and crosslinks. The mixing rule of T_g for binary miscible blends can be described by the Fox equation:

$$\frac{1}{T_g (\text{°K})} = \frac{w_1}{T_{g,1} (\text{°K})} + \frac{w_2}{T_{g,2} (\text{°K})} \quad (2)$$

where $T_{g,i}$ and w_i are glass transition temperature and weight fraction of component i ($i = 1$ or 2), respectively. Note that the unit of T_g is °K instead of °C for Equation 2. When the difference between $T_{g,1}$ and $T_{g,2}$ is relatively small compared to values of $T_{g,1}$ and $T_{g,2}$, the Fox equation can be approximated by a linear mixing rule:

$$T_g = w_1 T_{g,1} + w_2 T_{g,2} \quad (3)$$

where the unit of T_g can be either °K or °C. Equation 3 reveals a generic linear relationship between T_g and component concentration, which is consistent with the correlation between T_g and crosslink density described by Equation 1. As discussed below, Equation 3 can also help to understand other effects on T_g .

2) Effect of aromaticity

Formulations 1, 4, 5, and 6 were designed to examine the effect of aromaticity (Table 1) at a fixed index of 100. M_c was carefully controlled at 360 g/mol to ensure a constant crosslink density, while the aromaticity increases from 29.5% to 36.3% due to the increase of average OH_v for the polyol blend. DMTA data in Figure 4 demonstrate that the increase of

aromaticity raised T_g from 127 °C to 151°C. Similar rubbery plateau moduli are consistent with a fixed crosslink density at similar cup foam density (7 pcf). Figure 5 further indicates a linear relationship between T_g and aromaticity (Ar):

$$T_g (\text{°C}) = 368.4Ar + 17.6 \quad (4)$$

This composition dependence is also consistent with the linear mixing rule described by Equation 3. Moreover, the combination of Equations 1 and 4 leads to the following correlation:

$$T_g (\text{°C}) = 38.334 \times 10^3 / M_c + 368.4Ar - 89.5 \quad (5)$$

which captures both effects of crosslink density and aromaticity for PU systems made from PO-based polyols and polymeric MDI at an index of 100. Either Equation 1 or 4 can be viewed as a reduced version of Equation 5 at a specific aromaticity or M_c . This simple empirical correlation will be verified by some samples shown below.

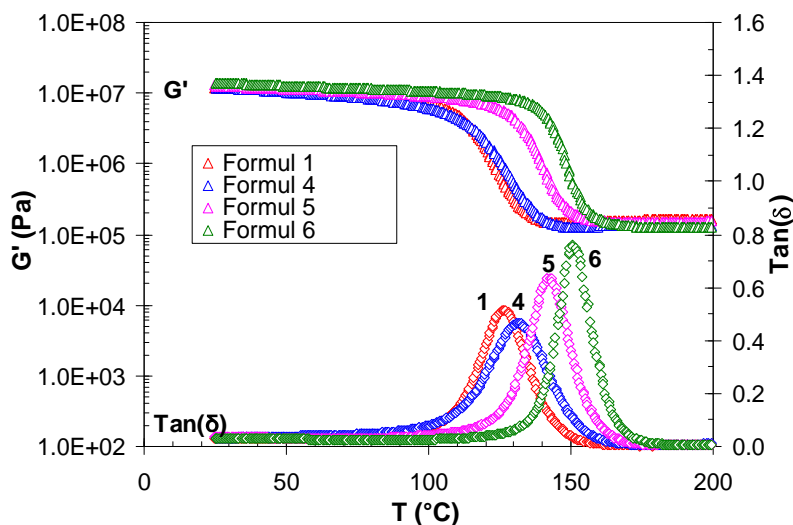


Figure 4. DMTA curves of Formulations 1 (red), 4 (blue), 5 (pink) and 6 (green).

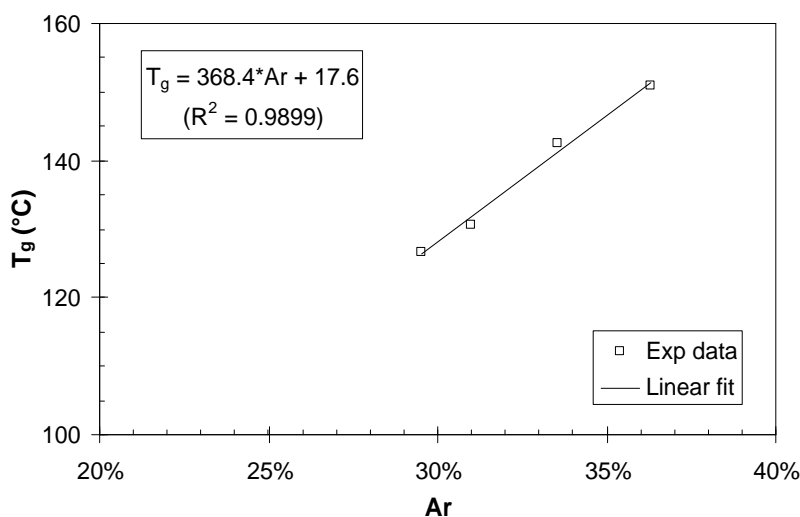


Figure 5. Glass transition temperature (T_g) as a function of aromaticity (Ar). Open squares denote experimental data, while solid straight line denotes linear fit of experimental data.

3) Effect of plasticizer

TCPP was chosen as a plasticizer because it has been widely used as flame retardant and viscosity reducer in PU rigid foam systems. Since TCPP exists as a non-reactive diluent in the rigid foam, it plasticizes the polymer matrix. As shown in Formulations 7 to 10 (Table 2), 0, 5 parts, 10 parts and 15 parts of TCPP were added into the polyol G to prepare foam with polymeric MDI. Figure 6 compares DMTA curves for these four formulations. Increasing concentration of TCPP gradually shifted the glass transition to lower temperature. Interestingly, Equation 5 can quantitatively capture this behavior, as shown in Figure 7. Without any TCPP, the measured T_g of Formulation 7 is the same as predicted by Equation 5. The addition of TCPP slightly swelled the network structure (i.e., elevated M_c) and diluted the aromaticity (Table 2); this dilution effect depressed the T_g linearly at 2.7 °C per 1wt% TCPP. Although other plasticizers were not tested in this work, based on this swelling mechanism, we expect no significant difference between TCPP and other plasticizers. Note that there is a limitation to use of Equation 5 on a plasticized network. We anticipate that this linear relationship works well until swelling equilibrium is reached. Swelling equilibrium defines the upper limit of plasticizer (or solvent) concentration that a certain crosslinked network structure can take up. Beyond this limit, the excess of plasticizer will be squeezed out from polymer matrix during curing of PU rigid foam. The equilibrium concentration of plasticizer depends on crosslink density and interaction between polymer matrix and plasticizer. These important factors should be considered when selecting a non-reactive diluent.

Formulations	7	8	9	10
Polyol G	96.2	96.2	96.2	96.2
TCPP		5.0	10.0	15.0
Catalyst I	2.0	2.0	2.0	2.0
Surfactant	1.0	1.0	1.0	1.0
Water	0.8	0.8	0.8	0.8
Index	100	100	100	100
OH_v (mgKOH/g)	528	503	480	459
w_{TCPP}	0	0.022	0.042	0.062
M_c (g/mol)	309	316	322	329
Aromaticity	33.6%	32.8%	32.1%	31.5%
T_g (°C)	159	154	147	142

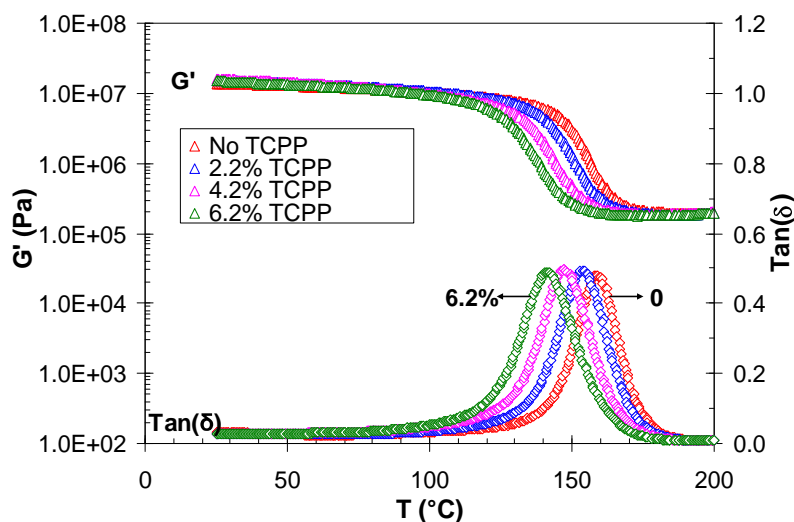


Figure 6. DMTA curves of Formulations 7 (red), 8 (blue), 9 (pink) and 10 (green) at various TCPP loadings.

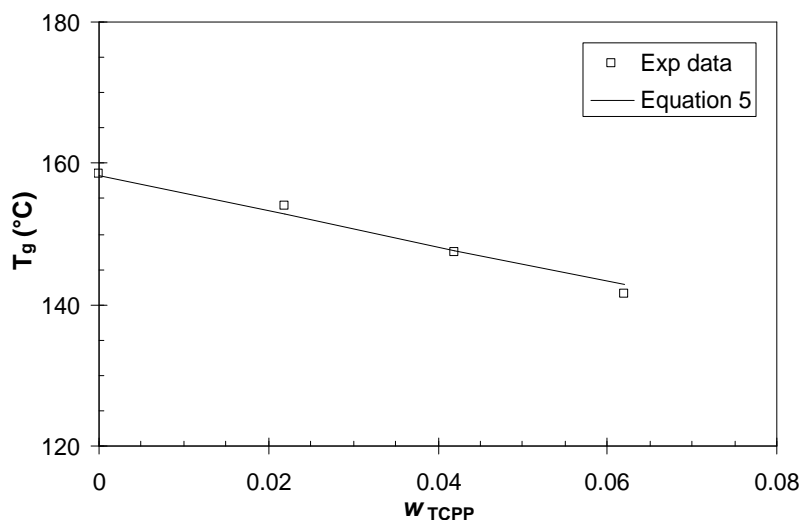


Figure 7. Glass transition temperature (T_g) as a function of weight fraction of TCP (W_{TCP}). Open squares denote experimental data, while solid straight line denotes prediction by Equation 5.

Table 3. Formulations 11 to 16 and their characteristics.

Formulations	11	12	13	14	15	16
Polyol A	96.2	96.2	96.2	96.2	96.2	96.2
Catalyst II	2.0	2.0	2.0	2.0	2.0	2.0
Surfactant	1.0	1.0	1.0	1.0	1.0	1.0
Water	0.8	0.8	0.8	0.8	0.8	0.8
Index	100	120	140	160	180	200
OH_v (mgKOH/g)	400	400	400	400	400	400
W_{PIR}	0	0.089	0.163	0.226	0.280	0.328
M_c (g/mol)	360	363	366	368	370	372
Aromaticity	29.5%	32.1%	34.4%	36.4%	38.0%	39.5%
T_g (°C)	131	143	153	164	179	189

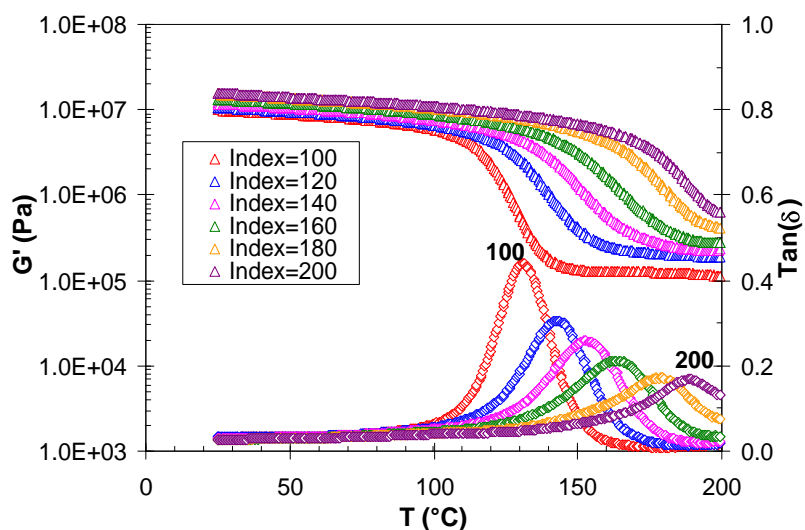


Figure 8. DMTA curves of Formulations 11 (red), 12 (blue), 13 (pink) 14 (green), 15 (yellow) and 16 (purple) at various indices from 100 to 200.

4) Effect of index

As index increases above 100, excess isocyanate groups can form, depending on catalysts and conditions allophanates, biurets or a PIR structure. Catalyst II containing a PIR catalyst was applied in Formulations 11 to 16 (Table 3) to promote primarily PIR formation. For this series of experiments, the same polyol blend was used with indices increasing from 100 to 200. Weight fraction of PIR (w_{PIR}) and M_c were calculated based on the assumption that all the excess of isocyanate groups were converted into PIR structure (Table 3). It is known from the literature that this assumption is only an approximation, because in real systems complete PIR conversion is difficult to achieve [5]. Figure 8 depicts the effect of index on DMTA curves. The increase in index moved T_g to higher temperature, while the peak of $Tan(\delta)$ became broader and lower. The width of $Tan(\delta)$ peak, or the temperature span of glass transition, can be associated with the heterogeneity of network structure. Wide $Tan(\delta)$ peak indicates a broad distribution of chain segment mobility. In other words, the increase of PIR content led to a broad distribution of PIR structure through the network structure: some regions contain more PIR content while some regions less. This morphology can be attributed to diffusion limitation during curing. Under a certain reaction exotherm, the formation of highly rigid PIR structure can dramatically slow down the mobility of unreacted isocyanate groups, leading to some PIR poor regions. This diffusion controlled curing kinetics has been observed for other highly crosslinked systems [6]. Figure 9 further illustrates a linear relationship between T_g and index:

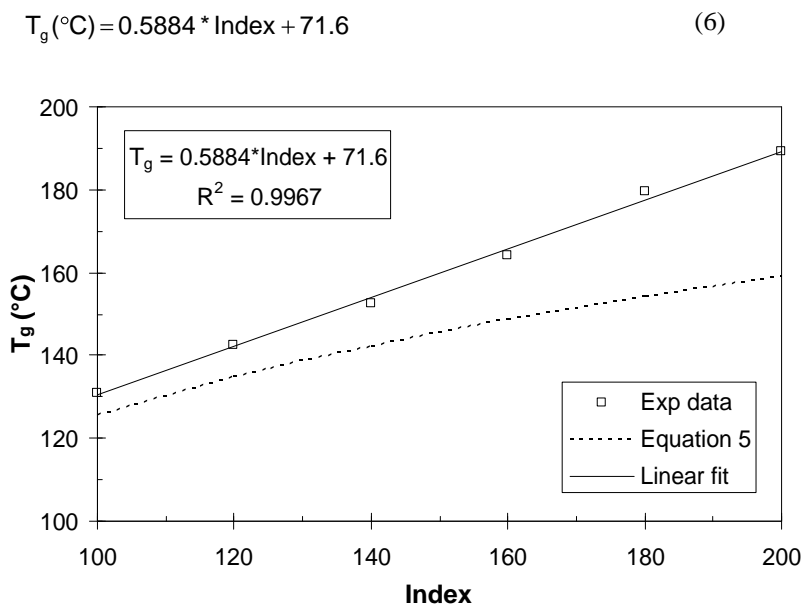


Figure 9. Glass transition temperature (T_g) as a function of index. Open squares denote experimental data, while solid straight line denotes linear fit of experimental data. The dot line represents the prediction of Equation 5.

Even though index is not proportional to the weight fraction of PIR (w_{PIR}), derivation based on the Fox equation indicates a linear correlation between index and the leading term of T_g , which dominates when the value of index is slightly higher than 1. Hence, large discrepancy can be expected when applying Equation 6 to systems whose indices are much greater than 200. In addition, the prediction by Equation 5 considerably underestimates the index effect on T_g (Figure 9). With the presence of PIR structure, T_g can not be simply correlated to crosslink density and aromaticity, as developed for 100 index PU systems. One strategy to solve this problem is to consider a high index system as a binary blend of PU and PIR components. The T_g of the PU component can be easily predicted by Equation 5 or measured for a 100 index system, while the T_g of the PIR component can be extrapolated using Equations 2 or 3. Figure 10 shows the best fitting curves of experimental data using either Equation 2 or 3. The Fox equation (i.e., Equation 2) fits the data slightly better than the linear mixing rule (i.e., Equation 3). However, both curves almost overlap at a PIR content lower than 0.4, while the Fox equation predicts a higher value of T_g than the linear mixing rule at higher PIR concentration. For a pure PIR structure ($w_{PIR} = 1.0$), $T_g = 396^{\circ}C$ (or $669^{\circ}K$) due to the Fox equation, and $306^{\circ}C$ due to Equation 3. Therefore, both mixing rules work well at relatively low PIR content. More effort is required to determine which mixing rule is better at very high indices.

In addition, it was realized that catalysts also play a role in the final glass transition temperature. The difference between Formulations 11 and 1 only lies in the catalysts: catalyst I versus catalyst II. Catalyst II containing a PIR catalyst led to $4^{\circ}C$ higher T_g compared to catalyst I. The increase of T_g can be attributed to the formation of some PIR structure catalyzed by the PIR catalyst even at 100 index. It should be emphasized that, besides PIR structure, other structures such as biurets,

allophanates and carbodiimides can also form due to the excess of isocyanate. The experimental data and correlations reflect overall effect of all these components.

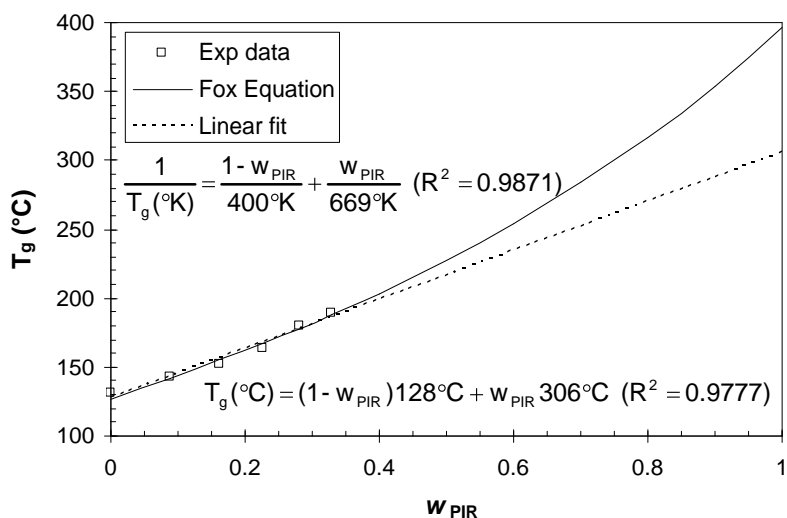


Figure 10. Glass transition temperature (T_g) as a function of weight fraction of PIR (w_{PIR}). Open squares denote experimental data. Solid and dot lines describe the best fit of experimental data with the Fox equation (Equation 2) and the linear mixing rule (Equation 3), respectively.

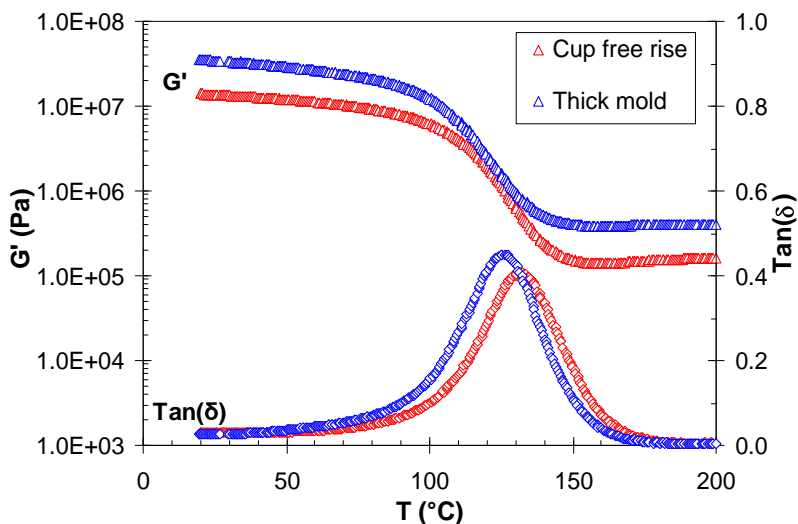


Figure 11. DMTA curves of a PU rigid foam system prepared in a 32oz cup (red) or molded in a 2.5 cm thick metal mold at 45 °C (blue). Molded density is two times higher than that of free rise foam.

5) Effect of processing

Besides those factors discussed above, the extent of curing can also affect the T_g of PU rigid systems. Although a complete conversion was assumed for the PU model system in this study, it might not be achievable under various real processing conditions [7]. For instance, Figure 11 illustrates that a particular PU rigid foam system exhibited different values in T_g when prepared in a 32oz cup or molded in a 2.5 cm thick metal mold at 45 °C (132 °C versus 125 °C). When mold thickness was reduced to 1 cm, T_g was further reduced to 116 °C (the first run curves in Figure 12). A much broader glass transition was also detected, which can be associated with post-curing during DMTA measurement. This was confirmed when a second run of DMTA was conducted for the same specimen. With a higher conversion, the $Tan(\delta)$ peak of second run became much narrower and shifted up to 128 °C, very close to T_g of the free-rise cup foam. As a highly crosslinked PU network, if the reaction temperature is not high enough, the reactive mixture will reach its apparent “ T_g ” at a

certain conversion such that further reaction is restricted due to poor mobility of unreacted functional groups. Therefore, the temperature profile due to mold temperature, reaction exotherm and heat transport can lead to a conversion profile across the mold thickness. The highest conversion is achieved in the center of mold due to the highest temperature. For the above study of the model system, under-cured samples were avoided by cutting DMTA specimen near the center of free-rise cup foam. This was also confirmed by the observation of two consecutive DMTA runs overlapping with each other (Data not shown). For real applications, mold temperature and reactivity of PU system have to be well designed to promote the conversion to completion [7].

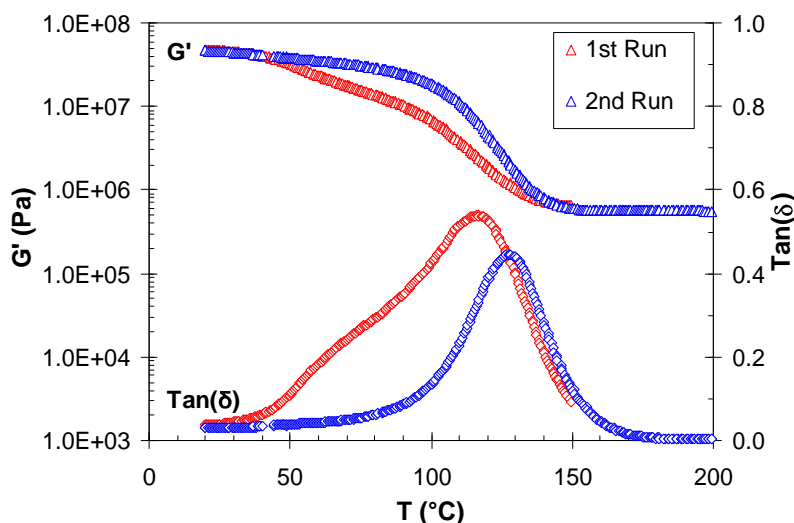


Figure 12. DMTA curves of a PU rigid foam system molded in a 1 cm thick metal mold at 45 °C. Red and blue curves denote the first run from 20 to 150 °C and the second run from 20 to 200 °C for the same specimen.

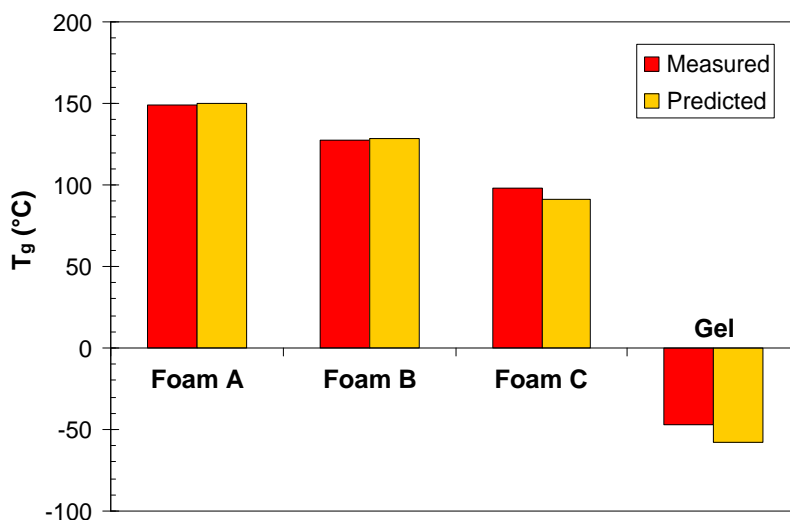


Figure 13. Comparison of T_g between DMTA measurement and prediction using Equation 5 for some representative examples of PU systems. Foams A and C were cut from free-rise cup foams, while Foam B and gel were sampled from parts.

6) Examples

Figure 13 compares measured T_g and prediction for four real examples of PU systems. Foams A and C were taken from free-rise cup foams, while foam B and a soft gel were sampled from molded parts. All four systems were based on various PO polyols and MDIs. Very good agreement was observed between measured and predicted values of T_g for rigid foams A and B. The T_g of foam C is 7 °C higher than the prediction. This can be attributed to the presence of a PIR catalyst in the

formulation of Foam C. PIR catalysts can result in higher T_g due to the formation of PIR structure, as discussed earlier (cf. Formulation 11). Surprisingly, even for a soft gel system, the discrepancy between measurement and prediction is only 11 °C. This suggests that the above correlations developed for the model PU rigid system can be further extended to PU gels.

The awareness of this structure-property relationship can dramatically accelerate the development of new systems, as exemplified below. For a certain rigid foam application, we need to adapt a formulation which has been well established in another country. The main challenge was how to replace some PO-based polyols which are not available in the US. This was easily achieved by matching crosslink density or M_c using US available products to ensure a similar network property. The new formulation was confirmed in several trials. For another application using high density PU rigid foam, after the window of T_g was defined, a new system was quickly formulated with cost-competitive raw materials using the above correlations. With some catalyst adjustment, it exhibited nice processing characteristics and final acceptable mechanical properties.

Some constraints should be underlined for these correlations. First of all, it only applies to a single phase system such as PU rigid and gel systems. Simple mixing rules of binary miscible blends will break down if there is phase separation between soft blocks and hard blocks. Secondly, those correlations were derived from a model PU rigid system based on PO polyols and polymeric MDI. For systems containing ethylene oxide (EO) based polyols and polyester polyols, the quantitative prediction might not work well, although linear composition dependence is expected to hold. New quantitative correlations can be established using a well designed model system formulated with those materials. In addition, the effect of PIR structure should be further explored for those systems too. Finally, the value of T_g in this work was determined by the peak of $\text{Tan}(\delta)$ of DMTA data at a certain frequency. As mentioned before, different characterization techniques or different frequencies can yield a range of T_g values. This factor should also be considered when applying these correlations.

CONCLUSION

A model PU rigid system was studied in terms of T_g , determined by rheology DMTA data. Correlations were developed between T_g and various structural factors including crosslink density, aromaticity, plasticizer and PIR structure (see Equations 1, 4, 5 and 6). The structure-property relationship is consistent with mixing rules for binary miscible blends (see Equations 2 and 3). Prediction by these correlations agreed very well with experimental data (Figure 13). In addition, rheology also revealed an effect of under-cured foam molded in thin molds (Figures 11 and 12), indicating the importance of processing in final conversion and properties. Finally, we demonstrated that the concept and relationship derived from this fundamental work could greatly accelerate the development of new PU rigid systems.

All information contained herein is provided "as is" without any warranties, express or implied, and under no circumstances shall the authors or Huntsman be liable for any damages of any nature whatsoever resulting from the use of reliance upon such information. Nothing contain in this publication should be construed as a license under any intellectual property right of any entity, or as a suggestion, recommendation, or authorization to take any action that would infringe any patent. The term "Huntsman" is used herein for convenience only, and refers to Huntsman Corporation, its direct and indirect affiliates, and their employees, officers, and directors.

REFERENCES

1. Dedecker, K. 2002. "Introduction to Rigid Foams," in *The Polyurethanes Book*, D. Randall, and S. Lee, eds. UK: Wiley.
2. Hiemenz, P. C. and T. P. Lodge. 2007. *Polymer Chemistry, 2nd Ed.* Boca Raton, FL: CRC Press.
3. Ferry, J. D. 1980. *Viscoelastic properties of polymers, 3rd Ed.* New York : Wiley.
4. Macosko, C. W. 1993. *Rheology : principles, measurements, and applications.* New York: VCH.
5. Lovenich, C. J. and B. Raffel. 2006. "A Quantitative Investigation of the Effect of the Recipe on the Trimer-yield in Polyisocyanurate Foams," *J. Cell. Plast.*, 42: 289
6. Lovell, L. G., K. A. Berchtold, J. E. Elliott, H. Lu, and C. N. Bowman. 2001. "Understanding the Kinetics and Network Formation of Dimethacrylate Dental Resins," *Polym. Adv. Technol.*, 12:335.
7. Macosko, C. W. 1989. *RIM: Fundamentals of Reaction Injection Molding.* New York: Hanser.

BIOGRAPHIES

Lifeng Wu



Lifeng Wu is currently a Senior Technical Specialist in the Americas Business Development Team of Huntsman at Auburn Hills, Michigan. Since joining in 2005, he has been involved in various projects including TPU, PU cast elastomers and rigid foams. He received his Ph.D. in Chemical Engineering from University of Minnesota in Minneapolis, M.S. and B.E degrees in Chemical Engineering from Tsinghua University in Beijing.

Janine Van Gemert



Janine Van Gemert is currently a Development Chemist in the Americas Business Development Team in Auburn Hills, Michigan. She has been involved in the development of thermoplastic polyurethanes, polyurethane rigid foam, and rheological characterization. Janine is currently finishing her Bachelor of Science in chemistry at Eastern Michigan University in Ypsilanti, Michigan. She is experienced in polyurethane, analytical, and archaeological chemistry.

Rafael E. Camargo



Rafael E. Camargo is currently the Elastomers Development Manager for the Americas Business Development Team in Auburn Hills, Michigan. He is responsible for new developments in multiple areas of polyurethane elastomers and related technologies. Dr. Camargo has over 20 years of experience in numerous polyurethane applications. He has been part of the Polyurethanes business at Huntsman since 1987 and has held a number of commercial and technical positions. Dr. Camargo has a Chemical Engineering Diploma from Universidad Pontificia Bolivariana in Medellin, Colombia and a Ph.D. in Chemical Engineering and Materials Science from the University of Minnesota in Minneapolis.

This work is protected by copyright. This paper and all data and information contained in it, are owned and protected by the ACC through its Center for the Polyurethanes Industry. Users are granted a nonexclusive royalty-free license to reproduce and distribute this paper, subject to the following limitations: (1) the work must be reproduced in its entirety, without alterations; and (2) copies of the work may not be sold. Copyright © Polyurethanes Technical Conference, American Chemistry Council.